MATERIALS PHYSICS AND MECHANICS RESEARCH ARTICLE

Submitted: September 22, 2025 **Revised: March 5, 2026** **Accepted: April 7, 2026**

Electrical properties of Nd doped barium zirconium titanate perovskite ceramics

Ch. Swathi [1], S.V. Jagadeesh Chandra [2]✉, B. Rajesh Kumar [2], Y. Srinivasa Rao [1], E.V. Krishna Rao [3], D.V. Rama Koti Reddy [1]

[1] Department of Instrument Technology, AU College of Engineering, Andhra University, Andhra Pradesh, India

[2] Thin Film and Nanotechnology Laboratory, Department of Physics, School of Science, GITAM (Deemed to be University), Andhra Pradesh, India

[3] Department of Electronics and Communication Engineering, Lakireddy Bali Reddy College of Engineering, Andhra Pradesh, India

✉ jsangara@gitam.edu

ABSTRACT

Barium zirconium titanate ceramics were prepared via the conventional solid-state reaction method. The influence of Nd^{3+} ion substitution on the ferroelectric and dielectric characteristics of barium zirconium titanate is investigated. To assess the thermal stability of Nd-doped samples, calcination was performed at temperatures of 1150, 1200, 1250, 1300, and 1350 °C for 4 h. The ferroelectric behavior of the doped ceramics was analyzed using polarisation-electric field hysteresis loops recorded at room temperature and 50 Hz, revealing improved energy storage density. Dielectric measurements, conducted over a frequency range of 1 kHz to 1 MHz with an impedance analyzer, indicated an increase in dielectric constant upon Nd addition. The BNZT-3 composition exhibited the highest remanent polarisation (P_r = 14.12 μC·cm^{-2}), highlighting its superior energy storage performance. Moreover, the materials demonstrated DC conductivity in the range of (1.26–8.37) × 10^{-6} S·m^{-1}, confirming enhanced electrical properties.

KEYWORDS

barium zirconium titanate • solid state reaction method • ferroelectric properties • dielectric properties

Citation: Swathi Ch, Jagadeesh Chandra SV, Rajesh Kumar B, Srinivasa Rao Y, Krishna Rao EV, Rama Koti Reddy DV. Electrical properties of Nd doped barium zirconium titanate perovskite ceramics. *Materials Physics and Mechanics*. 2026;54(3): 85–92.
http://dx.doi.org/10.18149/MPM.5432026_7

Introduction

Functional composite materials have potential applications in several fields due to their combination of multiple materials, which they also have individually [1–3]. In particular, it was widely used in piezoelectric transducers, DRAMs (dynamic random-access memories), electrical energy storage units and tunable microwave devices, and biomedical applications [4–8]. Among various multifunctional materials, barium titanate ($BaTiO_3$)-based compositions have received significant attention in the search for lead-free ferroelectric materials [9–14]. Barium zirconium titanate (BZT) attracts researchers' attention over barium strontium titanate (BST) for the fabrication of ceramic capacitors due to the greater chemical stability of Zr^{4+} compared with Ti^{4+} [15,16]. In general, complex perovskites have the formula (AA^1) (BB^1) O_3 and exhibit both ordered/disordered structures,

© Ch. Swathi, S.V. Jagadeesh Chandra, B. Rajesh Kumar, Y. Srinivasa Rao, E.V. Krishna Rao, D.V. Rama Koti Reddy, 2026.
Publisher: Peter the Great St. Petersburg Polytechnic University
This is an open access article under the CC BY-NC 4.0 license (https://creativecommons.org/li-censes/by-nc/4.0/)

which are basically relaxor ferroelectric materials [17,18]. Among various relaxor materials, BZT attracts researchers' attention for storage applications [19]. Various dopants have been added to the BZT system to enhance its dielectric properties [20]. Impurity doping is a common approach to improve a material's physical and electrical properties [6]. The addition of rare-earth ions to BZT influences the dielectric properties. Doped BZT ceramics have demonstrated potential applications not only for storage but also for microwave applications [21,22]. Considering the potential applications of barium-based solid solutions for electronic devices and the role of various dopants, the objective of the current research was to study the structural and initial dielectric behaviour of the BZT system by doping with neodymium (Nd). The structural properties of Nd-doped BZT ceramics were reported elsewhere [23]. The incorporation of neodymium (Nd^{3+}) into barium zirconium titanate (BZT) is used to improve it's dielectric and ferroelectric properties. Nd^{3+} ions substitute for the A-site (Ba^{2+}) cation in the perovskite lattice, causing lattice distortion and charge compensation, which enhances polarisation and energy storage capability. Due to differences in ionic radius and charge, the miscibility limit of Nd^{3+} in BZT is typically low, typically a few mol. %. Therefore, in this study, the Nd concentration was kept within this limit to maintain a single-phase perovskite structure and stable electrical properties.

Systematic studies on the influence of Nd substitution, ferroelectric behaviour, dielectric response, and electrical conductivity are still limited. In particular, the ferroelectric energy-storage performance of Nd-doped BZT has not been clearly correlated with structural and dielectric changes. The frequency-dependent dielectric response and direct current (DC) conductivity of Nd-doped BZT ceramics across different processing temperatures remain insufficiently reported. The present study addresses these gaps by analysing ferroelectric properties via P–E hysteresis loops, revealing enhanced remnant polarisation and improved energy-storage density. A comprehensive understanding of electrical transport behaviour is provided by evaluating DC conductivity. In this investigation, it is reported the effect of Nd content on the electrical properties of BZT, supported by ferroelectric hysteresis loops and dielectric characterization.

Materials and Methods

$(Ba_{1-x}Nd_{2x/3})(Zr_{0.3}Ti_{0.7})O_3$ (x = 0.05, 0.10, 0.15, 0.20 and 0.25 %) ceramics were prepared by the conventional solid state reaction method with reagents commercial high purity powders (M/S Loba Company) of $BaCO_3$ (99.9 %), ZrO_2 (99.9 %), TiO_2 (99.9 %) and Nd_2O_3 (99 % pure, SRL) were weighed according to their stoichiometric ratio. The powders grinded in a high energy planetary mono model ball mill, which contains 250 ml tungsten carbide jar and tungsten balls (8 mm dia and 8 g/m^2) by maintaining the ratio of powder to ball as 1:2. In this grinded process, toluene C_7H_8 (M.W 92.14 g/mol, 99 % pure, SRL) as binding medium for 12 h continuously with a rotational speed of 200 rpm, with a short break of 10 min after every 30 min, of grinding to cool down the machine temperature. Conventional calcinations were performed on the dried powders in a box furnace at 1500 °C. Initially, neodymium (Nd) was doped 0.05 % to the barium zirconium titanate (BZT) and calcined at 1150, 1200, 1250, 1300 and 1350 °C for 4 h. The sample calcinated at 1350 °C showed better structural properties than those at the other mentioned

temperatures. For further confirmation, the calcination process was performed for 2, 4, and 6 h at the same temperature. The samples were calcined for 4 h at 1350 °C, which predominantly confirms the BZT peaks in the X-ray diffraction (XRD) spectra [23]. Since the samples calcinated at 1350 °C for 4 h showed sharp peaks, the remaining samples doped with Nd at 0.10, 0.15, 0.20, and 0.25 % were calcinated at 1350 °C for 4 h. Calcination of each sample was followed by heating in an air oven at 80 °C to dry the sample. An air-dry silver paste is applied to the polished pellet surfaces to form the electrodes. The samples were electrically poled in a silicon oil bath at 100 °C by applying a dc field of 20 kV/cm to measure ferroelectric properties with polarisation-electric field loop tracer (Marine India). The electrode samples were characterized for the dielectric constant (ε), and the dissipation factor (tan δ) using a 1260A Impedance Analyzer.

Results and Discussion

Ferroelectric *P-E* loops analysis

Figure 1 shows the polarisation-electric field (P–E) hysteresis loop of pure and Nd doped BZT ceramic samples at room temperature, measured under a constant frequency of 50 Hz. The pure and Nd-doped (0.05, 0.10, 0.15, 0.20 and 0.25 %) BZT ceramics were named BZT, BNZT-1, BNZT-2, BNZT-3, BNZT-4 and BNZT-5, respectively. As the main focus was on the Nd-dopant effect on the ferroelectric properties of the undoped sample (BZT), here the discussion focuses only on the doped samples. In particular, as there is no variation in the ferro-electric properties, such as remnant polarisation (P_r), maximum polarisation (P_{max}), and coercive field (E_c) obtained from the *P-E* loops of BNZT-1 and BNZT-2 and BNZT-4 and BNZT-5, here we disseminate only BNZT-1, 3 and 5 samples. It has been observed that the lower P_r value for BNZT-1 may be due to polar nanoregions formed by broken global symmetry, which suppress ferroelectricity. It can be noted that the values of P_r and P_{max} increase and reach the maximum values of 14.12 and 25.08 μC/cm^2 by increasing the Nd dopant concentration upto 0.15 % (BNZT-3). A possible explanation for this observation is that the addition of Nd^{3+} ions reduces

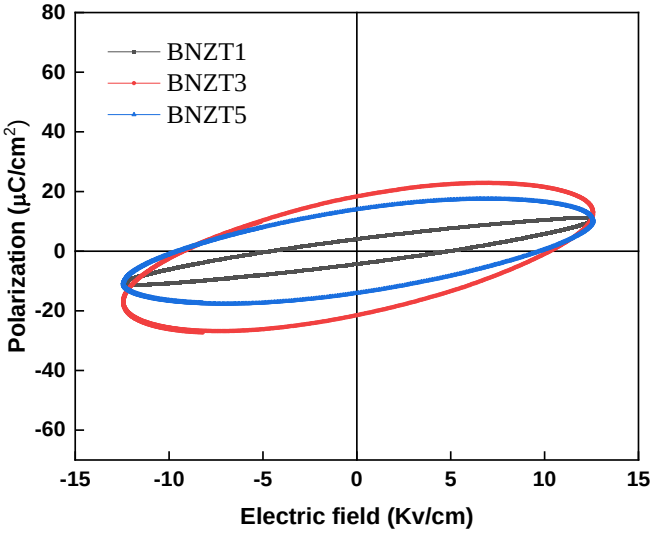


Fig 1. Ferroelectric hysteresis loop of pure and Nd doped BZT ceramic

barium volatility, thereby enhancing the stability of the metal–oxygen site in BZT and decreasing domain pinning due to oxygen vacancies [24]. The rise P_r with increasing electric field is explained as the poling voltage increases: more domains with higher activation energy are activated in the dynamic process, and more switched domains are frozen in the switched state after the electric field is removed. Since the activated domains have higher activation energy, a larger electric field E_c is required to switch these domains back. The maximum values of P_r can also be attributed to a high dielectric constant, as evidenced by the dielectric study, which eases the nucleation and growth of polar nano regions [25].

The significantly large grain size could also be responsible for the high remnant polarisation in BNZT-3. The higher P_r value (14.12 μC/cm^2) with lower coercive field (E_c = 3.78 kV/cm) for BNZT-3 is due to the composition residing at the phase boundary between tetragonal and cubic structures. The lower E_c value indicates that the domain moves more easily, suggesting that reduced energy loss during the electric-field sweep enhances the ferroelectric properties [26]. The improved ferroelectric behaviour in BNZT-3 is mainly due to the structural transition, which lowers the O-Ti-O bond angle, helping to increase the vibration and diffusion of the off-centred octahedral Ti ion and neighbouring oxygen ions. However, with a further increase Nd, particularly in the case of BNZT-5 samples, the P_r and E_d values were relatively lower than those of BNZT-3. The reduced remnant and coercive field values can be due to the increase in the gain size with increasing Nd dopant concentration. The polarisation and coercive field values obtained from the P-E loops are shown in Table 1. The relatively higher value of the difference between P_{max} and P_r (P_{max}-P_r) for the BNZT-3 sample, compared with BNZT-1 and BNZT-5, might be due to the enhancement of energy storage density [26]. Generally, the combination of relatively high P_{max} observed in BNZT-3 indicates an optimized balance between energy density and efficiency [27,28]. These results clearly demonstrate that compositional modification significantly influences ferroelectric behavior and enhances the suitability of BNZT-3 for energy storage capacitor applications.

Table 1. Remnant polarization (P_r), maximum polarization (P_{max}), and coercive field (E_c) values for pure and Nd doped BZT

Sample	P_r, μC/cm^2	E_c, kV/cm	P_{max}, μC/cm^2	E_{max}, kV/cm	P_{max}-P_r, μC/cm^2
BNZT-1	4.18	2.433	11.223	12.509	7.04
BNZT-3	14.12	3.776	25.076	10.885	10.95
BNZT-5	8.84	3.343	17.444	11.556	8.60

Dielectric properties

Figure 2 shows the frequency-dependent (0.001–1 MHz) dielectric constant measurements for pure and Nd-doped BZT samples at room temperature. The escalation of dielectric constant at lower frequencies is mainly due to increased space charge and interfacial polarisation. At low frequencies, the dielectric constant was observed to be high due to space-charge polarisation at grain boundaries, which generates a potential barrier. Then, an accumulation of charge at the grain boundary led to higher values of the real part of the permittivity. The dielectric dispersion can be explained by the dominance

of the grain boundary effect rather than the grains. It was attributed to Maxwell–Wagner-type interfacial polarisation in accordance with Koop's phenomenological theory.

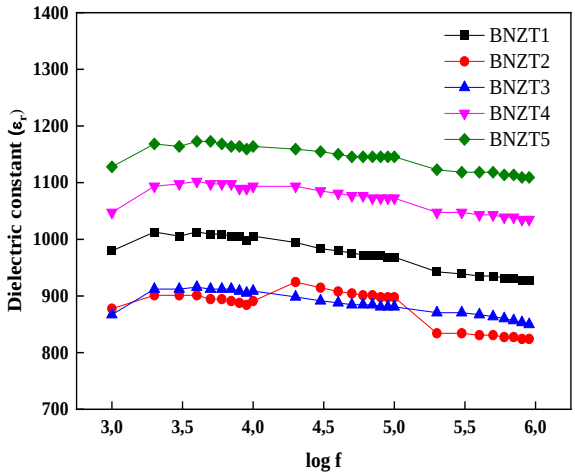


Fig. 2. Frequency-dependent dielectric constant for Nd doped BZT samples

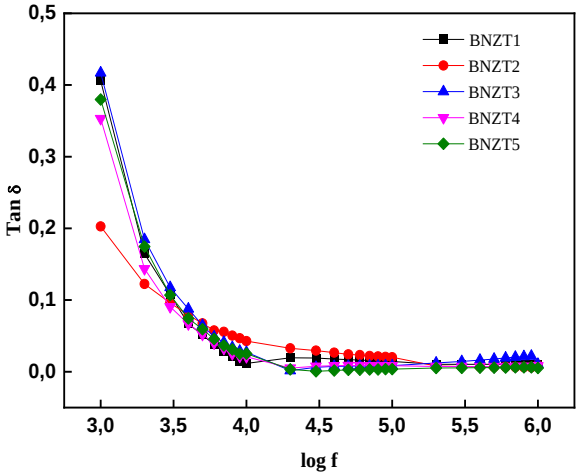


Fig. 3. Frequency dependent dielectric loss tangency for Nd doped BZT samples

The dielectric loss tangent (tan (δ)) is related to the dielectric relaxation process and is given as the ratio of the imaginary ε'' and the real part ε', i.e., $\tan(\delta) = \varepsilon''/\varepsilon'$. Dielectric loss represents energy loss and occurs when polarisation shifts behind the applied electric field due to grain boundaries. Figure 3 shows the frequency dependence of dielectric loss tangent $(Ba_{1-x}Nd_{2x/3})(Zr_{0.3}Ti_{0.7})O_3$ (x = 0.05, 0.10, 0.15, 0.20 and 0.25) ceramic. In general, the dielectric loss of dielectric materials arises from three distinct factors: space-charge migration (interfacial polarisation), direct current (DC) conduction, and low-resistivity grains separated by thin, poorly conducting grain boundaries. Under the applied electric field, the localised charge accumulation is observed, leading to molecular dipole motion (dipole loss).

To explain the decrease in the real part of permittivity at higher frequencies, we assumed that the dielectric structure is composed of interfacial polarisation. The high value of tan(δ) at low frequencies can be attributed to the greater dominance of grain-boundary resistivity over grain resistivity, leading to increased energy loss [29].

Figure 4 shows the frequency dependence of AC conductivity for $(Ba_{1-x}Nd_{2x/3})(Zr_{0.3}Ti_{0.7})O_3$ (x = 0.05, 0.10, 0.15, 0.20 and 0.25) ceramics. At the high-frequency end, the curves approach each other, once again indicating the possibility of space charges. A basic fact about the carrier's conductivity is that σ increases with frequency (any hopping model has this feature). The observed frequency-independent σ_{dc} is explained by the relaxation jump model [30]. According to this model, at low frequencies and/or higher temperatures, conduction occurs via hopping of charged particles between localised states, resulting in long-range translational motion of charge. At first glance, it appears that σ spectra can be split into two zones: the first is at low frequencies, where σ is not significantly frequency-dependent, showing a plateau correlated with the DC conductivity. The second one is at higher frequencies, where σ increases with frequency. According to the Jonscher universal power law [31] the conductivity is calculated:

$$\sigma_{ac}(\omega) = \sigma_{dc} + A\omega^n, \quad (1)$$

where $\sigma_{ac}(\omega)$ and σ_{dc} have the usual meaning, A is a constant, and n is the power exponent that can take values less than 1 [32]. The transport mechanism was explained by the thermally activated hopping process between two sites separated by an energy barrier. Equation (1) was used to fit the conductivity data. In the fitting procedure, A and s values were varied simultaneously to obtain the best fits. The frequency exponent (n) in BNZT ceramic is less 1, indicating non-Debye behaviour and translational motion of charge carriers via a hopping mechanism. The Jonscher power law fitting results of conductivity for $(Ba_{1-x}Nd_{2x/3})(Zr_{0.3}Ti_{0.7})O_3$ (x = 0.05, 0.10, 0.15, 0.20 and 0.25 wt. %) samples are shown in Table 2.

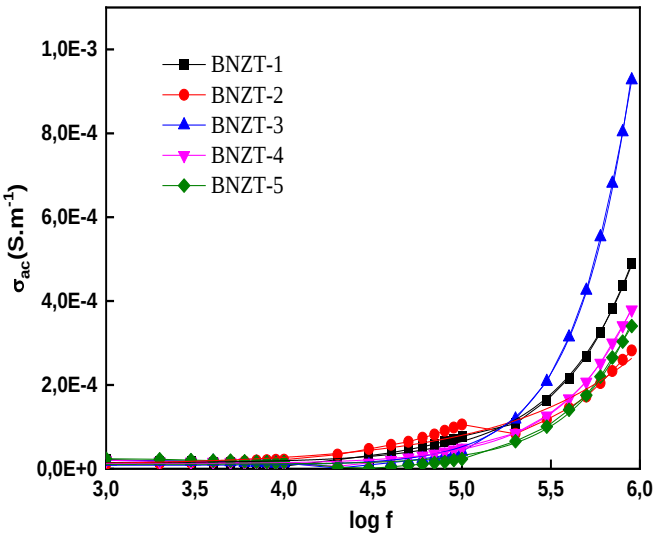


Fig. 4. Frequency dependent AC conductivity for Nd doped BZT samples

Table 2. The Jonscher power law fitting results from AC conductivity

Sample	σ_{dc}, 10^{-6} (S·m^{-1})	A, 10^{-10}	n
BNZT1	2.28	4.41	0.43
BNZT2	7.74	8.98	0.75
BNZT3	8.37	5.12	0.31
BNZT4	1.26	1.41	0.40
BNZT5	2.47	1.11	0.34

The incorporation of neodymium (Nd^{3+}) into barium zirconium titanate (BZT) ceramics significantly influences the AC conductivity, dielectric, and ferroelectric properties. The Nd^{3+} ions generally substitute at the A-site (Ba^{2+}) of the perovskite lattice by creating lattice distortion and charge imbalance. This substitution leads to the formation of oxygen vacancies or defect dipoles, which enhance charge-carrier mobility and, consequently, increase AC conductivity. At low to moderate Nd concentrations, the defect concentration increases in a controlled manner by improving charge-hopping mechanisms and polarisation behaviour, thereby enhancing AC conductivity. However, when the Nd concentration becomes too high, excessive defect formation may occur, leading to incrased leakage current, lattice disorder, and deterioration of ferroelectric polarisation. Therefore, an optimal Nd-doping level exists at which AC conductivity was enhanced without significantly degrading dielectric and ferroelectric performance.

Conclusions

Barium zirconium titanate (BZT) ceramics doped with neodymium (Nd^{3+}) were successfully synthesized using the conventional solid-state reaction method. The *P–E* hysteresis measurements at 50 Hz demonstrated enhanced ferroelectric behaviour with Nd doping, with the sample BNZT-3 exhibiting the maximum remnant polarisation (P_r) of 14.12 μC·cm^{-2}, suggesting improved energy storage capability. Frequency-dependent dielectric studies (0.001–1 MHz) showed an increase in the dielectric constant with increasing Nd substitution. Additionally, the prepared ceramics exhibited DC conductivity in the range of (1.26–8.37) ×10^{-6} S·m^{-1}. The results confirm that Nd^{3+} doping significantly improves the ferroelectric and dielectric performance of BZT ceramics, making them promising candidates for energy storage and electronic device applications.

CRediT authorship contribution statement

Chanamolu Swathi is fully responsible for preparing all types of samples and for most of the analyses conducted in this research work. **Sangaraju Venkata Jagadeesh Chandra**, **Borra Rajesh Kumar**, and **Ede Venkata Krishna Rao** are responsible for the entire analytical part of the research work. **Yarravarapu Srinivasa Rao** and **Dodda Venkata Rama Koti Reddy** fully guided the entire investigation and all aspects of the analysis of this work.

Conflict of interest

The authors declare that they have no conflict of interest.

References

1. Bernevig BA, Felser C, Beidenkopf H. Progress and prospects in magnetic topological materials. *Nature.* 2022;603: 41–51.
2. Abdelhamid HN. An introductory review on advanced multifunctional materials. *Heliyon.* 2023;9: e1806.
3. Kim Y, Zhao X. Magnetic soft materials and robots. *Chem. Rev.* 2022;122(5): 5317.
4. Gutkin MY, Skiba NV. Emission of lattice dislocations from triple junctions of grain boundaries in high-temperature ceramics with amorphous intracrystalline layers. *Materials Physics and Mechanics.* 2024;52(1): 39–48.
5. Vaiani L, Boccaccio A, Uva AE, Palumbo G, Piccininni A, Guglielmi P, Cantore S, Santacroce L, Charitos IA, Ballini A. Ceramic Materials for Biomedical Applications: An Overview on Properties and Fabrication Processes. *J. Fun. Biomater.* 2023;14(3): 146.
6. Naik BG, Chandra SVJ, Uthanna S. Influence of oxygen partial pressure on the structural, optical and electrical properties of magnetron sputtered $Zr_{0.7}Nb_{0.3}O_2$ films. *Appl. Phys. A.* 2021;127: 979.
7. Kondaiah P, Chandra SVJ, Fortunato E, Choi CJ, Rao GM, Reddy DVRK, Uthanna S. Substrate temperature influenced ZrO_2 films for MOS devices. *Sur. Int. Ana.* 2020;52(9): 541–546.
8. Chandra SVJ, Fortunato E, Martins R, Choi CJ. Modulations in effective work function of platinum gate electrode in metal-oxide-semiconductor devices. *Thin Solid Films.* 2012;520(14): 4556–4558.
9. Sufiiarov V, Kantyukov A, Popovich A, Sotov A. Structure and properties of barium titanate lead-free piezoceramic manufactured by binder jetting process. *Materials.* 2021;14(16): 4419.
10. Belov AYu. Subcritical growth of repolarization nuclei in polycrystalline ferroelectric Films. *Materials Physics and Mechanics.* 2024;52(1): 18–25.
11. Yao K, Chen S, Lai SC, Yousry YM. Enabling Distributed Intelligence with Ferroelectric Multifunctionalities. *Adv. Sci.* 2022;9(1): 2103842.

12. Bhargavi GN, Badapanda T, Khare A. An investigation of structural, electrical and optical properties of lead-free barium zirconium titanate (BZT)-based ceramic compounds. *Phase Transitions.* 2021;94(6–8): 474–492.
13. Lin X, Zhao X, Zhou L, Zhao M, Lin Y, Yao Y, Liang B, Tao T, Lu SG. Novel barium zirconate titanate-based lead-free ceramics with stably high energy storage performance over a broad temperature and frequency range. *J Mater Sci: Mater Electron* 2021;32: 11845–11856.
14. Abhijeet V, Shahaji PD, Tejas KK, Birajdar RJJ, Nalam PG, James AR, Kolekar YD, Ramana CV. High-Performance, Lead-Free Magnetoelectric Composites Based on Nickel–Cobalt Ferrite and Calcium/Zirconium-Substituted Barium Titanate. *ACS Applied Engineering Materials*. 2024;3(1): 142–157.
15. Tang XG, Chew KH, Chan HLW. Diffuse phase transition and dielectric tunability of $Ba(Zr_yTi_{1-y})O_3$ relaxor ferroelectric ceramics. *Acta Mater.* 2004;52(17): 5177–5183.
16. Ghosh SK, Ganguly M, Rout SK, Chanda S, Sinha TP. Structural, optical and dielectric relaxor properties of neodymium doped cubic perovskite $(Ba_{(1-x)}Nd_{2x/3})(Zr_{0.3}Ti_{0.7})O_3$. *Solid State Sci.* 2014;30: 68–77.
17. Sagar R, Madolappa S, Raibagkar RL. Electrical, dielectric and pyroelectric behavior of neodymium substituted barium zirconium titanate. *Solid State Sci.* 2012;14(2): 211–215.
18. Aktaş PS. Structural investigation of barium zirconium titanate $Ba(Zr_{0.5}Ti_{0.5})O_3$ particles synthesized by high-energy ball milling process. *J. Chem. Sci.* 2020;132(1): 130.
19. Maiti T, Guo R, Bhalla AS. Enhanced electric field tunable dielectric properties of $BaZr_xTi_{(1-x)}O_3$ relaxor ferroelectrics. *Appl. Phys. Lett.* 2007;90(18): 182901
20. Reddy SB, Rao KP, Rao MSR. Effect of La substitution on the structural and dielectric properties of $BaZr_{0.1}Ti_{0.9}O_3$ ceramics. *J Alloys Comp.* 2009;481(1–2): 692–696.
21. Sagar R, Hudge P, Madolappa S, Kumbharkhane AC, Raibagkar RL. Electrical properties and microwave dielectric behavior of holmium substituted barium zirconium titanate ceramics. *Journal of Alloys and Compounds.* 2012;537: 197–202.
22. Ali A, Uddin S, Lal M, Zaman A, Iqbal Z, Althubeiti K. Structural, optical and microwave dielectric properties of $Ba(Ti_{1-x}Sn_x)_4O_9$, $0 \leqslant x \leqslant 0.7$ ceramics. *Scientific Reports.* 2021;11: 17889.
23. Swathi C, Sangaraju VJC, Rao YS, Reddy DVRK. Influence of Nd dopant on the Structural properties of barium zirconium titanate perovskite. *ZastitaMaterijala.* 2025;66(2): 233–239.
24. Srimathy B, Jayavel R, Bhaumik I, Ganesamoorthy S, Karnal AK, Gupta PK, Kumar J. Role of dopant-induced defects on the properties of Nd and Cr doped PZNT single crystals. *Mater. Sci. Eng. B.* 2014;185: 60–66.
25. Shreya M, Radhapiyari L, Singh KC. Improved electric properties of lead-free neodymium doped $Ba_{0.85}Ca_{0.15}Zr_{0.1}Ti_{0.9}O_3$ piezoceramics. *Mater. Res. Bullet.* 2018;105: 253–259.
26. Reda M, Ei-Dek SI, Arman MM. Improvement of ferroelectric Properties via Zr doping in barium titanate particles. *J Mater Sci: Mater. Electron.* 2022;33: 16753–16776.
27. Nguyen MD. Ultrahigh energy-storage performance in lead-free BZT thin-films by tuning relaxor behavior. *Mater Res Bullet.* 2021;133: 111072.
28. Ribeiro DJM, Nair SKP, Jayakrishnan AR, Oliveira J, Magagnin G, Albertini D, Walter Y, Sekhar KC, Agostinho Moreira J, Almeida BG, Gautier B, Vilquin B, Marques L, Pereira M. Silva JPB. Engineering Pb-free relaxor ferroelectric thin films for low voltage energy storage applications. *Nanoscale.* 2025;17: 19794–19805.
29. Thanamoon N, Chanlek N, Moontragoon P, Srepusharawoot P, Thongbai P. Microstructure, low loss tangent, and excellent temperature stability of Tb^+ Sb-doped TiO_2 with high dielectric permittivity. *Results in Physics.* 2022;37: 105536.
30. James AR, Srinivas K. Low temperature and impedance spectroscopy of PMN-PT. *Ceramics: Mater. Res. Bull.* 1999;34: 1301–1310.
31. Jonscher AK. *Universal Relaxation Law*. London: Chelsea Dielectrics Press; 1996.
32. Zeydi I, Zaidi A, Dhahri J, Zaidi MA, Elhabradi M. Frequency and temperature dependent dielectric properties in the lead-free $Ba_{0.75}Ce_{0.033}Sr_{0.2}Ti_{0.96}Sn_{0.04}O_3$ ceramics. *Applied Physics A.* 2019;125: 656.